Variations of Lake Ice Phenology on the Tibetan Plateau from 2001 to 2017 Based on MODIS Data

Yu Cai[1,2,3], Chang-Qing Ke[1,2,3,4,*], Xingong Li[5], Guoqing Zhang[6], Zheng Duan[7], Hoonyol Lee[8]

1. School of Geography and Ocean Science, Nanjing University, Nanjing, 210023, China
2. Jiangsu Provincial Key Laboratory of Geographic Information Science and Technology, Nanjing University, Nanjing, 210023, China
3. Key Laboratory for Satellite Mapping Technology and Applications of State Administration of Surveying, Mapping and Geoinformation of China, Nanjing University, Nanjing, 210023, China
4. Collaborative Innovation Center of Novel Software Technology and Industrialization, Nanjing, 210023, China
5. Department of Geography and Atmospheric Science, The University of Kansas, Lawrence, KS 66045-7316, USA
6. Institute of Tibetan Plateau Research, Chinese Academy of Sciences, Beijing,100101, China
7. Technical University of Munich, Munich, 80333, Germany
8. Division of Geology and Geophysics, Kangwon National University, Chuncheon, Kangwon-do 24341, Republic of Korea

[*]Corresponding author: Chang-Qing Ke (C. Q. Ke, kecq@nju.edu.cn)
Tel: 0086-25-89685860
Fax: 0086-25-83592686

Key Points:

- Lakes in the northern Inner Tibetan Plateau (Inner-TP) have longer ice cover durations than those in the southern Inner-TP.
- 18 lakes have extending ice cover durations (avg. 1.11 d yr^{-1}) and 40 lakes have shortening durations (avg. 0.80 d yr^{-1}).
- Lake ice phenology is influenced by climatic conditions, geographical location, and the physico-chemical characteristics of the lakes.

Abstract

Lake ice is a robust indicator of climate change. The availability of information contained in Moderate Resolution Imaging Spectroradiometer (MODIS) daily snow products from 2000 to 2017 could be greatly improved after cloud removal by gap filling. Thresholds based on open water pixel numbers are used to extract the freeze-up start and break-up end dates for 58 lakes on the Tibetan Plateau (TP), 18 lakes are also selected to extract the freeze-up end and break-up start dates. The lake ice durations are further calculated based on freeze-up and break-up dates. Lakes on the TP begin to freeze-up in late October and all the lakes start the ice cover period in mid-January of the following year. In late March, some lakes begin to break-up, and all the lakes end the ice cover period in early July. Generally, the lakes in the northern Inner-TP have earlier freeze-up dates and later break-up dates (i.e. longer ice cover durations) than those in the southern Inner-TP. Over 17 years, the mean ice cover duration of 58 lakes is 157.78 days, 18 (31%) lakes have a mean extending rate of 1.11 d yr^{-1} and 40 (69%) lakes have a mean shortening rate of 0.80 d yr^{-1}. Geographical location and climate conditions determine the spatial heterogeneity of the lake ice phenology, especially the ones of break-up dates, while the physico-chemical characteristics mainly affect the freeze-up dates of the lake ice in this study. Ice cover duration is affected by both climatic and lake specific physico-chemical factors, which can reflect the climatic and environmental change for lakes on the TP.

Key Words: Lake ice phenology; Freeze-up/break-up dates; Climate change; MODIS; Tibetan Plateau

1 Introduction

There are about 1200 lakes (>1 km^2) on the Tibetan Plateau (TP) (Zhang, Yao, Xie, Zhang, K., et al., 2014) and many studies have shown that lake ice phenology (i.e., the timing of freeze-up, break-up and duration of ice cover) responds well to climatic and environmental changes (Brown & Duguay, 2010; Weber et al., 2016). As "the Third Pole of the Earth", the TP is very sensitive to global climate change (Liu & Chen, 2000; Qiu, 2008; Kang et al., 2010). Changes in air and water surface temperatures related to climatic changes are important factors in the lake ice phenology changes (Adrian et al., 2009; Zhang, Yao, Xie, Qin, et al., 2014; Dörnhöfer & Oppelt, 2016; Yao et al., 2016). At the same time, the state and type of lake ice and their change to open water system in turn affects the local or regional climate (Rouse et al., 2005; Brown & Duguay, 2010). Freeze-up/break-up processes can result in sudden changes in lake surface properties (such as albedo and roughness), which affect the energy exchange between the lake water and the atmosphere (Latifovic & Pouliot, 2007). Therefore, in the context of global climate change, lake ice phenology can be used as a good indicator to monitor the actual impact of climate change on lakes and their surroundings (Ke et al., 2013).

However, due to the harsh environment and limited accessibility, few meteorological stations exist in the central and western TP, which is where lakes are concentrated; thus, it is difficult to carry out field observations. These factors result in a lack of continuous and complete historical records on regional climate changes (Liu & Chen, 2000; Kropacek et al., 2013). Remote sensing data have been widely used in lake ice monitoring (Wei & Ye, 2010; Duguay et al., 2015). Passive microwave sensors such as the Scanning Multichannel Microwave Radiometer (SMMR), the Special Sensor Microwave/Image (SSM/I), and the Advanced Microwave Scanning Radiometer for the Earth Observing System (AMSR-E) have high temporal resolutions (at times twice daily or better) and are suitable for monitoring lake ice changes in large lakes, such as Qinghai Lake (Che et al., 2009; Cai et al, 2017) and Nam Co (Ke et al, 2013) on the TP, and Great Bear Lake and Great Slave Lake (Howell et al., 2009) in Canada. However, there are still many medium- and small-size lakes on the TP, which are smaller than the pixel size of passive microwave images (dozens to hundreds of km^2). Active microwave sensors have high spatial resolutions (1 m to about 100 m). For example, the European Remote Sensing Satellite (ERS)-1/2 Synthetic Aperture Radar (SAR) has been used for monitoring the lake ice formation process and ice thickness (Jeffries et al., 1994; Morris et al., 1995; Duguay & Lafleur, 2003). Radarsat-1/2 SAR has also been used for monitoring the freeze-up/break-up processes of lake ice (Duguay et al., 2002; Geldsetzer et al., 2010). However, the low temporal resolution (five to six days) of the available active microwave technologies limits the ability to achieve daily monitoring on lake ice (Latifovic & Pouliot, 2007; Chaouch et al., 2014). The medium- and high-resolution optical data, such as Moderate Resolution Imaging Spectroradiometer (MODIS) and Advanced Very High Resolution Radiometer (AVHRR) obtain daily images and are often used to monitor lake freeze-up/break-up dates and areas. For example, Weber et al. (2016) used AVHRR data to extract the ice phenology of European lakes in different climatic regions. Yao et al. (2016) used MODIS and Landsat data to extract the ice phenology of 22 lakes in the Hoh Xil region from 2000 to 2011 and analyzed the factors influencing lake ice changes. Chaouch et al. (2014) used MODIS data to monitor the growth and regression of ice in the Susquehanna River in the northeastern USA. However, optical images are obscured by clouds, which limits the direct usage of optical data (Gafurov & Bárdossy, 2009). Currently, there have been many mature cloud removal methods, including methods based on temporal and spatial continuity (Gafurov & Bárdossy, 2009; Paudel & Andersen, 2011; López-

Burgos et al., 2013) and methods combining multiple sensor data (Liang et al., 2008; Gao, Xie, Lu, et al., 2010; Gao, Xie, Yao, et al., 2010), which can reduce cloud cover and increase data availability by gap filling approaches and compositing.

The unique geographical and climatic conditions of the TP make it a region of high interest for climate research (Kang et al., 2010). Owing to the low annual air temperature, many lakes on the TP have long and stable ice cover periods during winter. Recent studies on individual lakes have shown that on the TP, the freeze-up dates of some lakes have been delayed, the break-up dates have advanced, and the ice cover durations have significantly shortened (Che et al., 2009; Ke et al., 2013; Cai et al., 2017). However, there are few ice phenology studies covering the entire TP. Guo et al. (2018) used MODIS reflectance data, eight-day synthetic snow product and land surface temperature data to analysis the uncertainty and variation of different remotely sensed lake ice phenology across the TP. Kropáček et al. (2013) used MODIS eight-day synthetic snow products to analyze the ice phenology changes of 59 large lakes on the TP from 2001 to 2010. However, the eight-day interval could not capture the lake ice phenology very precisely, especially for the start and end dates of freeze-up and break-up. To date, no one has used MODIS daily snow products to study the lake ice phenology on the TP.

To obtain the lake ice phenology variations on the TP, the daily snow products of MODIS are used to extract the freeze-up and break-up dates of lake-wide ice cover from 2001 to 2017. The lake ice durations are then calculated, and the spatial variabilities and change rates of lake ice phenology are analyzed. Using reanalysis data and available satellite data set, the effects of air temperature, lake surface water temperature, and wind speed on lake ice phenology are analyzed. In addition, possible influence of geographical determined lake locations and physico-chemical conditions on lake ice phenology are also investigated.

2 Study area

The TP is located in central Asia; it is the largest plateau in China, and its elevation is the highest in the world. The TP is known as the “roof of the world” and “the Third Pole of the Earth”, with an average elevation of over 4,000 m a.s.l and a total area of approximately 3.0 million km^2 (Qiu, 2008; Zhang et al., 2013). There are about 1,200 lakes (>1 km^2) on the TP with a total size of 47,000 km^2, which accounts for more than 50% of the total size of Chinese lakes (Zhang, Yao, Xie, Zhang, K., et al., 2014), in which 389 lakes have an area larger than 10 km^2, including three lakes larger than 1,000 km^2: Qinghai Lake (4,254.9 km^2), Selin Co (2,129.02 km^2) and Nam Co (2,040.9 km^2) (Wan et al., 2014).

By analyzing the change of ice coverage for each lake using MODIS daily snow products, 58 lakes with a stable ice cover period (less cloud cover, less pixel misclassification and obvious ice cover period) are manually selected as study lakes (Figure 1), including three lakes larger than 1,000 km^2, 35 lakes larger than 100 km^2 and 20 lakes smaller than 100 km^2, in which the smallest lake is Xuemei Lake (41.33 km^2, Wan et al., 2014). Most lakes (>70%) are in the Inner basin (Zhang et al., 2013). To analyze the spatial variability of lake ice phenology, the Inner basin is divided into upper and lower parts (Inner I and Inner II, northern and southern parts of about 33°N) (Zhang et al., 2013), and lakes outside the Inner basin are classified as Other III (Figure 1). The lake masks used were extracted from Landsat images (Wan et al., 2014) and all data sets involved in the extraction and comparisons are clipped by the same lake mask. An annual period extends from 1 August to 31 July of the following year, for example, 1 August 2012 to 31 July 2013 is noted as the annual period of 2013.

3 Data and methods

3.1 Data

3.1.1 MODIS daily snow cover products

MODIS is mounted on the Terra and Aqua satellites, which obtain global observation data every one or two days. The available daily snow cover products with a spatial resolution of 500 m from MODIS include MOD10A1 (Terra) and MYD10A1 (Aqua). The available temporal range of MOD10A1 is from 1 August 2000 to 31 July 2017 and that of MYD10A1 is from 1 August 2002 to 31 July 2017. Four MODIS tiles (h24v05, h25v05, h25v06 and h26v05) cover the 58 lakes of this study. The data were obtained from the US National Snow and Ice Data Center (http://nsidc.org/, Version 5 for 2001-2016 and Version 6 for 2017) on 8 September 2017.

The accuracy of the daily snow cover products of MODIS are approximately 93% under clear sky conditions (Maurer et al., 2003; Parajka & Blöschl, 2006; Hall & Riggs, 2007; Sorman et al., 2007; Huang et al., 2011). However, the daily snow cover products over the TP have a yearly average cloud cover (>40%) from MODIS observations (Yu et al., 2016), and need to be processed for cloud removal by gap filling. Some lakes may have snow covering the ice surface during the ice cover period, and MODIS snow cover products could classify these ice covered pixels into snow covered pixels, which results in a low lake ice cover compared to the lake size (Kropacek et al., 2013). Therefore, the changes of lake water cover proportions (the number of lake water pixels divided by the total number of pixels within the lake boundary) are used to extract the freeze-up/break-up dates, and the lake ice cover proportions are used to assist in correcting the date results. Under clear sky conditions, the reduction in water cover is considered as the result of lake ice cover increase.

3.1.2 Landsat data

The Landsat program is a series of Earth observing satellites, which is co-managed by the National Aeronautics and Space Administration (NASA) and the United States Geological Survey (USGS) to monitor earth and environmental resources. Since 23 July 1972, eight satellites have been launched including Landsat Multispectral Scanner (MSS, ~80 m) and Thematic Mapper (TM, 30m)/Enhanced Thematic Mapper Plus (ETM+, 30m)/Operational Land Imager (OLI, 30 m) with a temporal resolution of 16 days. Landsat data used are from the standard USGS Landsat Surface Reflectance products (Collection 1 Level-2) of Landsat 5, 7 and 8 from 2000 to 2017 on the Google Earth Engine platform (https://earthengine.google.com/). Images without cloud cover and obtained during the freeze-up or break-up periods are selected to extract the lake water cover proportions.

To extract lake ice, pixels covering a lake need to be first distinguished from other types of pixels, such as cloud and land. A threshold of 0.4 for Normalized Difference Snow Index (NDSI) (Hall et al., 2001) is applied to extract the extent of a lake as follows:

$$NDSI = (TM\ Band\ 2 - TM\ Band\ 5) / (TM\ Band\ 2 + TM\ Band\ 5) \geq 0.4 \qquad (1)$$

Then, according to the actual reflectance of each image, different thresholds on the near-infrared band are set to distinguish lake ice from lake water. Finally, the proportion of lake water within a lake boundary (1 – ice cover proportion) is calculated and compared with MODIS results on the same day to verify the accuracy of using MODIS snow cover products after cloud removal by gap filling.

3.1.3 Lake ice phenology products from AMSR-E/2 data

The daily lake ice phenology time series derived from AMSR-E and AMSR2 by Du et al. (2017) provide 5 km ice phenology retrievals describing daily lake ice conditions over the Northern Hemisphere (http://files.ntsg.umt.edu/data/AMSRE2_LAKE_ICE_PHEN/). The date set is used for lake-wide comparisons against MODIS data results from 2003 to 2011 and from 2013 to 2015. Pixels within the lake boundary are extracted for eight lakes larger than 500 km^2. Considering the differences between passive microwave and optical data and the difference in data productions, when the number of ice-on pixels count for more than 10% of all pixels in the lake, the date is determined to be freeze-up start date, and less than 10% is break-up end date.

3.1.4 Reanalysis meteorological data

The NCEP/NCAR reanalysis data set is a joint product from the National Centers for Environment Prediction (NCEP) and the National Center for Atmospheric Research (NCAR, https://www.esrl.noaa.gov/). This data set provides reanalysis meteorological data every six hours including air temperature, air pressure, relative humidity, and wind speed at a spatial resolution of 2.5° from 1 January 1948 to present. The monthly mean data of near surface air temperature and wind speed are used.

To match the annual ice period, the annual mean air temperature and wind speed are calculated from August of the current year to July of the following year. Then, the change rates of air temperature and wind speed from 2001 to 2017 are calculated. Finally, the inverse distance weighted (IDW) method is used to interpolate and calculate the means and change rates of air temperature and wind speed for each lake over the 17 years.

3.2 Methods

3.2.1 Cloud removal for the MODIS snow product

The cloud removal (gap filling) process has two steps. The first step is to combine daily Terra and Aqua snow cover products to determine lake cover type (Gafurov & Bárdossy, 2009). For a pixel *A*, if any of the pixels on Terra or Aqua images for the same day is open water (or other useful pixel types such as ice and snow, the same below), the pixel on the output image is determined to be covered by water. When the pixel is covered with clouds (or other useless types such as land and missing data, the same below) on both Terra and Aqua images, the output pixel is determined to be cloud covered (Gafurov & Bárdossy, 2009):

$$S_{(A,\ output)} = water \text{ if } S_{(A,\ Aqua)} = water \text{ OR } S_{(A,\ Terra)} = water \tag{2}$$

$$S_{(A,\ output)} = cloud \text{ if } S_{(A,\ Aqua)} = cloud \text{ AND } S_{(A,\ Terra)} = cloud \tag{3}$$

Since Aqua satellite was launched in 2002, there is no first step data process for the 2001-2002 period. The images from step one are used as the inputs for the following step. The second step is based on the temporal correlation of cloud cover pixels (Gafurov & Bárdossy, 2009). First, if a pixel *A* on date *t* is cloud covered, the pixels on the images of previous and next days will be searched, and if both pixels are water covered, pixel on date *t* is determined to be covered by water as follows (Gafurov & Bárdossy, 2009):

$$S_{(A,\ t)} = water \text{ if } S_{(A,\ t-1)} = water \text{ AND } S_{(A,\ t+1)} = water \tag{4}$$

If pixel *A* on date *t-1* is cloud covered, then the pixel on date *t-2* will be searched, and if both pixels on date *t-2* and date *t+1* are water covered, the pixels on date *t* and *t-1* will be replaced by water. Similarly, if the pixel on date *t+1* is cloud covered, the pixel on date *t+2* will be searched as follows (Gafurov & Bárdossy, 2009):

$$S_{(A,\, t-1)}, S_{(A,\, t)} = water \text{ if } S_{(A,\, t-2)} = water \text{ AND } S_{(A,\, t+1)} = water \tag{5}$$

$$S_{(A,\, t)}, S_{(A,\, t+1)} = water \text{ if } S_{(A,\, t-1)} = water \text{ AND } S_{(A,\, t+2)} = water \tag{6}$$

3.2.2 Extraction of freeze-up/break-up dates

Often, there will be an unfrozen area near a lake's outlet during the freeze-up period, and a small amount of accumulated lake ice on the lakeshore during the break-up process (Reed et al., 2009; Yao et al., 2016). In addition, repeated freeze-up and break-up periods caused by weather changes, mismatch of lake boundaries, misclassification of pixels and inevitable noise (especially cloud cover) will all change the extraction of lake ice phenology. Therefore, Kropacek et al. (2013) proposed using 5% and 95% of the lake area as thresholds to extract ice phenology instead of 0% and 100%. Simultaneously, images with a cloud cover of more than 50% over a lake after gap filling are eliminated to reduce the influence from sudden changes in water cover.

First, a median M of all the lake water cover proportions in a year is calculated. Then, all the water cover proportions are divided into two groups: one group (G_h) contains the values greater than M, and the other group (G_l) contains the values less than M, and the mean values of both groups are calculated. Two thresholds are determined by using the 5% and 95% of the two mean values as follows (Kropacek et al., 2013):

$$Th_h = 95\% \cdot M_h + 5\% \cdot M_l \tag{7}$$

$$Th_l = 5\% \cdot M_h + 95\% \cdot M_l \tag{8}$$

Where M_h and M_l are the mean values of group G_h and G_l, respectively. Since the freeze-up/break-up processes of lakes are usually short, M_h can represent the typical proportion of a lake covered by water during the non-ice cover period, and M_l can represent the typical water cover proportion during ice cover period (Kropacek et al., 2013). The dates when the water cover will no longer raise above the thresholds (Th_h for freeze-up start date and Th_l for freeze-up end date) again during the freeze-up period and will no longer drop below the thresholds (Th_l for break-up start date and Th_h for break-up end date) during the break-up period are extracted as the ideal lake ice phenology dates. Sometimes the remained cloud cover (or other useless pixels) will decrease the water cover (even smaller than the thresholds). Therefore, after the automatic extraction, the extracted dates need to be checked again by visual interpretation of the complete water, ice and cloud cover changes within a year (Figure 2).

The four freeze-up/break-up dates divide the annual status of a lake into four periods and the corresponding durations can be calculated: freeze-up duration (FUD, from freeze-up start to freeze-up end), break-up duration (BUD, from break-up start to break-up end), complete freezing duration (CFD, from freeze-up end to break-up start) and ice cover duration (ICD, from freeze-up start to break-up end).

3.2.3 Statistical analysis

The mean absolute error (MAE), correction of determination (R^2) and bias are measured for comparisons between the MODIS cloud-removed and Landsat data as well as comparisons between ice phenology results derived from MODIS and passive microwave data sets. Trend significances of lake ice dates and durations are evaluated using the non-parametric Mann-Kendall test (Mann, 1945; Kendall, 1975). Furthermore, the relationships between lake ice phenology parameters and climate conditions are evaluated using the coefficient of correlation (r).

4 Results

4.1 Cloud removal of MODIS snow cover products and validation using Landsat data

4.1.1 Cloud removal by gap filling

Taking the year 2013 as an example, before gap filling, the mean cloud cover of the 58 lakes is 44.97% and 51.70%, respectively, for Terra and Aqua. After the first step of combining the data from two satellites, the cloud cover is eliminated to 31.02%. After the second step of using pixels in neighboring dates, the mean cloud cover is eliminated to 16.54%. Taiyang Lake has a mean cloud cover of more than 60%, which is the highest among 58 lakes, and it is eliminated to 35.49% after the cloud removal. For some lakes, the cloud cover can even be eliminated to less than 5% after cloud removal (Table 1). For example, the mean cloud cover of Qinghai Lake in 2013 after cloud removal is 7.54%, and the freeze-up/break-up dates can be clearly distinguished (Figure 2).

4.1.2 Validation

For some large lakes, such as Qinghai Lake, Landsat images cannot cover the entire lake on the same day and images acquired from different days cannot be mosaiced to extract the lake ice. Often, the freeze-up/break-up period of a lake is only a dozen of days, which is usually not captured by Landsat images due to the 16-day temporal resolution. In addition, considering the influence of cloud cover, there are indeed few available Landsat images. Therefore, lakes which can be covered by one Landsat image and those with relatively long freeze-up/break-up period are preferably selected for validation.

A total of 28 Landsat images covering Nam Co (19 images) and Selin Co (9 images) during the freeze-up or break-up periods are selected. The proportions of lake water to total lake area are calculated for each image and compared with the water cover proportions from the cloud removed MODIS data. The R^2 is 0.95, the mean absolute error (MAE) is 4.58% and the bias is 2.09% (Figure 3), indicating a relatively high accuracy and MODIS data can be used to detect lake water changes well after cloud removal.

4.2. Comparisons against other lake ice data sets

Daily passive microwave brightness temperature data, including AMSR-E/2 and SSM/I, are used for cross-validation with MODIS lake ice phenology results. The freeze-up start and break-up end dates of eight lakes (larger than 500 km^2) derived from AMSR-E/2 pixel-level lake ice phenology products (Du et al., 2017) from 2003 to 2015 (except 2012) are compared with corresponding MODIS dates and the results are shown in Table 2. The break-up end dates from two data sets are strongly correlated (avg. R^2 = 0.90) but the freeze-up start dates have relatively low consistency (avg. R^2 = 0.35). Generally, MODIS dates are earlier than AMSR dates, but vary from lake to lake (Table 2). The MAEs of freeze-up start dates range for eight lakes from 2.92 to 7.25 days and break-up end dates range from 1.75 to 3.25 days.

Furthermore, ice phenology data for Qinghai Lake (from 2001 to 2016, Cai et al., 2017) and Nam Co (from 2001 to 2013, Ke et al., 2013) derived from SSM/I data are also compared with MODIS results. The correlations of freeze-up start and break-up end dates for Nam Co are low (R^2 = 0.42 and 0.35, respectively) and the MAEs are both over six days (Table 2). The freeze-up start date from MODIS data is obviously earlier than SSM/I data (bias = -5.28 days), this may be because Nam Co only covered by two SSM/I pixels and less information can be provided. On the other hand, Qinghai Lake provided four freeze-up/break-up dates for comparison against MODIS data. Similar to AMSR results, the consistency of freeze-up dates are lower than break-up dates (Figure 4). Moreover, in Qinghai Lake, freeze-up dates from MODIS data are earlier than passive microwave data (both SSM/I and AMSR) while break-up dates are later (Figure 4), this may be because of the coarser spatial resolution and less information near the boundary of passive microwave data (Cai et al., 2017). The MAE of freeze-up end date is the largest (6.56 days) and the MAEs of break-up dates are about two days (Figure 4). These results indicate that the influence from different remote sensing data and different data production processes on freeze-up dates may be larger than that on break-up dates. It is similar to the results of Du et al. (2017) when he compared AMSR lake ice phenology results against Canadian Ice Service (CIS) and IMS data.

4.3. Ice phenology and its change of the lakes on the TP from 2001 to 2017

For each of 58 lakes, freeze-up start and break-up end dates are extracted, and their corresponding ice cover durations are calculated. Some lakes do not freeze-up completely in winter due to mild winters, large water volume and/or high salinity (Kropacek et al., 2013), and some lakes are obscured by cloud and/or misclassified pixels during ice cover period. Apart for these lakes, for 18 lakes with characteristic change of water cover proportions, the freeze-up end and break-up start dates are also extracted, and four lake ice durations (i.e., freeze-up duration, break-up duration, complete freezing duration and ice cover duration) are calculated, such as Har Lake in Figure 5. Based on the four freeze-up/break-up dates and four durations from 2001 to 2017, their mean values and change rates of ice phenology for the 58 lakes are shown in Appendix Table A1. Additional statistics are shown in Appendix Table B1 and Table 3.

4.3.1 Freeze-up/break-up dates

Around late October, Yuye Lake has begun to freeze-up, which is the earliest among 58 lakes. After Taro Co had begun to freeze-up by mid-January of the following year, all the lakes on the TP have started their ice cover periods. The gap between freeze-up start dates among the lakes can be as long as three months. From late March to early July, the lakes have ended their ice period one after another, and the earliest and latest lakes are Tuosu Lake and Gozha Co, respectively. Generally, the spatial difference in the freeze-up dates are smaller than the break-up dates (Table B1). The mean freeze-up start date for the lakes in the Inner I is 32.68 days earlier than that of the lakes in the Inner II, while the mean break-up end date in the Inner I is 43.56 days later than that in the Inner II (Figure 6, Table 3).

Freeze-up/break-up dates for many lakes on the TP have obvious change tendencies from 2001 to 2017 (Table A1). For example, the freeze-up start and freeze-up end dates for Har Lake have been delayed at a rate of 0.66 d yr^{-1} and 0.35 d yr^{-1}, respectively, and the break-up start and break-up end dates have advanced at rates of 0.38 d yr^{-1} and 0.12 d yr^{-1}, respectively (Figure 5). Overall, the change rates of freeze-up dates for most lakes are more significant than the break-up dates (Table A1). Except for a few lakes in the eastern Inner I which have advancing trends in the freeze-up dates, most of the lakes (81.03%) show delayed trends from 2001 to 2017. All the lakes in the Inner II have delayed trends during the 17 years (Figure 6b, Table 3). Among the 58 lakes, the lakes with delayed and advancing trends of break-up dates are both 50% (Table 3). Spatially, the delayed trend is more pronounced than the advancing trend (Figure 6d). Lakes in the Inner I, such as Dogaicoring Qangco and Lexiewudan Co (change rates of the break-up end dates are 3.50 d yr^{-1} and 4.25 d yr^{-1}, respectively, Table A1), experienced the most dramatic changes (Figure 6d). During the 17 years, 60.34% of the lakes show an opposite change trend of freeze-up and break-up dates, and another 36.21% of the lakes show the same delayed change trend. Only Huolunuo’er and Meiriqiecuomari have the same advancing trend of freeze-up and break-up dates (Table A1).

4.3.2 Lake ice durations

Lake ice cover durations on the TP differ greatly, where the duration of the shortest lake (Taro Co) is less than three months, and that of the longest lake (Xuemei Lake) is approximately eight months (Table B1). The spatial distribution of the ice cover duration is consistent with that of the freeze-up/break-up dates: the lakes in the Inner II with later freeze-up and earlier break-up have shorter ice cover durations, and the lakes in the Inner I with earlier freeze-up and later break-up have longer ice cover durations (Figure 7a), which is 2 months longer on average than those of the Inner II (Table 3). Among the 18 lakes extracted complete four freeze-up/break-up dates, most lakes (72.2%) have shorter freeze-up durations than break-up durations, i.e., freeze-up takes place faster than break-up does (Table A1). However, the variations in freeze-up durations among the lakes is larger than that in break-up durations (Table B1). Among the 18 lakes, Hoh Xil Lake has the earliest freeze-up end date and the latest break-up start date; thus, the longest complete freezing duration is up to seven months. Qinghai Lake has the shortest complete freezing duration of less than three months (Table B1).

Over the 17 years, most of the lakes (68.97%) display a shortening trend in ice cover duration. For example, Har Lake has a shortening trend of 0.77 d yr^{-1} (Figure 5d). Lakes with extending trends are mainly concentrated in the eastern part of the Inner I (Figure 7b). Since all the lakes in the Inner II have delayed trends of freeze-up start dates, most lakes (87.50%) have their ice cover durations shortened. Similar to freeze-up/break-up dates, half of the lakes in the Inner I have shortening ice cover durations and the other half have extending durations (Table 3). The trends of complete freezing duration for the 18 lakes are mainly consistent with the trends of ice cover duration. Lakes such as Hoh Xil Lake and Tu Co have a shortening freeze-up and break-up durations, despite an expending ice cover duration. Although lakes such as Dagze Co and Ngangze Co have shortening trends of ice cover duration, their shortening freeze-up and break-up duration results in an extending trend of complete freezing duration. 77.78% of the lakes show the same trend in freeze-up and break-up durations (Table A1). There are several lakes, such as Har Lake, which have shortening freeze-up durations and extending break-up durations (Figure 5c). The freeze-up and break-up durations of most lakes (both 72.2%) have shortened over 17 years, which indicates that freeze-up/break-up takes place faster (Table A1).

5 Discussions

5.1 Uncertainty analysis

Errors in the extraction of the ice phenology from MODIS snow cover products mainly come from three aspects: (1) The MODIS snow cover products have cloud cover, misclassification and occasional missing data; (2) changes to the original data caused by cloud removal; and (3) misjudgment when extracting the lake ice phenology dates. While the quality of MODIS snow cover products cannot be changed, the proportion of usable pixels can be increased by removing some of the cloud cover by gap filling. Combining Terra and Aqua data can solve the problem of missing dates, and combined with the temporal information of cloud (noise) covered pixels, about two-thirds of the cloud and other noise pixels can be eliminated. Cloud cover could reflect most of the solar radiation, so the cloud cover in a short period of time would not have much impact on lake surface coverage (Gafurov & Bárdossy, 2009). Possible increased lake ice caused by snowfall during cloudy days (or low temperature at night) are ignored if they break-up on the following sunny day (or in the daytime). According to the study of Gafurov and Bárdossy (2009), the performance accuracy of the gap filling approach is more than 95%. To maintain with the original MODIS information as much as possible, the cloud-removal process only considers the temporal information one to two days before and after the current day, and the potential error can be controlled within two days. Although the possible error in the gap filling process is minimized, the remained and persistent (longer than two days) cloud cover will still influence the extraction of ice phenology dates.

The remained cloud cover (or other useless pixels) will decrease the lake water/ice cover of the day, and sometimes the automatic extraction method may obtain a wrong date. However, these mistakes can be modified by later manual correction of comparing the complete water/ice/cloud curves of that year. Using thresholds can control the difficulty caused by repeated freeze-up and break-up of lake ice and ensure the consistency of the freeze-up/break-up date extractions. For example, there were several periods of repeated freeze-up and break-up at the start of the break-up process in Qinghai Lake in 2013. It is difficult to determine which break-up date should be extracted without using a threshold. Though the extracted date seems like a wrong date, the ice cover has definitely dropped after that day, so the date is determined to be the break-up date of that year (Figure 2). Although some dates will be checked and modified after automatic extraction, the alternative dates are all selected by the thresholds. Considering the existence of noise, the thresholds are set to 5% and 95% instead of the extreme values. This approach may cause the later extraction of the freeze-up start and break-up start dates, and earlier of the freeze-up end and break-up end dates. But without available validation data, the actual error cannot be accurately evaluated. However, the same rule is applied to all the lakes and in all the years, which makes the comparisons between lakes and years possible.

The persistent cloud cover is difficult to be eliminated. But similarly, without surface observation data, the errors cannot be accurately evaluated. It seems some lakes have the feature that cloud covered most areas during freeze-up and/or break-up periods. However, lakes with too much noise or complex shape (for example, Bangong Co is long and narrow and Yamzho Yumco is tentacle-like) that cannot guarantee the reasonable dates has already been excluded in the lake selection period. Furthermore, some lakes have persistent cloud cover after they begin to freeze-up, it is probably caused by misclassification of ice to cloud. If the cloud cover influences the extraction of the freeze-up end and/or break-up start date, the dates will not be extracted. Only lakes with clear curves of water/ice changes are chosen in order to obtain more accurate dates, even if the cost is that the number of the study lakes will be reduced.

Kropáček et al. (2013) extracted the lake ice phenology of 59 large lakes on the TP from 2001 to 2010 using MODIS eight-day synthetic snow products. The lakes were divided into three groups, among which the lakes in Group C were almost all located in the Inner II. The mean ice cover duration of lakes in Group C was 126 days with a shortening trend of 1.6 d yr^{-1}, while the mean ice cover duration of lakes in the Inner II in this study is 128 days from 2001 to 2017, and the mean change rate of 21 lakes is -0.89 d yr^{-1}. The two mean ice cover durations are similar, the change trends are consistent, and the lower rate in this study may be caused by gentler change in recent years. Yao et al. (2016) used MODIS and Landsat data to study lake ice phenology in the Hoh Xil region from 2000 to 2011. Their mean ice cover duration was 196 days with a mean change rate of -1.91 d yr^{-1}. The Hoh Xil region is in central Inner I, and the lakes analyzed in their study include Dogaicoring Qangco, Taiyang Lake, Hoh Xil Lake, Lexiewudan Co, and Margai Caka. This is the region where lake ice phenology has changed drastically in recent years within the TP (Figure 6). Consistent with the results of this study, Dogaicoring Qangco and Lexiewudan Co are the rare lakes in this region with advancing freeze-up dates and delayed break-up dates, and the reason for these changes will be discussed in the following section. However, in this study, the freeze-up start and break-up end dates of Taiyang Lake have been delayed over 17 years, which is different from an advancing break-up end date in Yao et al. (2016). From 2000 to 2011, the break-up end date of Taiyang Lake did show an advancing trend with a rate of 1.51 d yr^{-1}. However, since 2010, the break-up end date has been delayed annually with a change rate of 3.23 d yr^{-1} until 2017, which results in an overall delayed trend from 2001 to 2017. Furthermore, many studies have shown that some large lakes on the TP such as Qinghai Lake and Nam Co show a significant delayed trend in freeze-up dates and an advancing trend in break-up dates, and the ice cover durations have shortened in recent years (Che et al., 2009; Ke et al., 2013; Cai et al., 2017), which is consistent with the results of this study.

5.2. Influencing factors on lake ice phenology

5.2.1. Climatic factors

The low spatial resolution of the reanalysis data makes it difficult to ensure that the IDW-interpolated air temperature/wind speed can represent the actual local situation for each single lake. However, the large-scale spatial distribution of meteorological factors and the change rates of the lakes over 17 years on the TP can be obtained from the data. In addition, available lake water surface temperature (LWST) data for 57 lakes (except for Youbucuo Lake in the Inner II) from 2002 to 2015 derived from MODIS Land Surface Temperature (LST) products by Wan et al. (2017) are used.

Compared to the Inner II, the Inner I has a lower mean annual air temperature, LSWT and wind speed from 2001 to 2017 (Table 4). Under relatively cold conditions with low wind speed, lakes in the Inner I have earlier freeze-up dates, later break-up dates and longer ice cover durations than do lakes in the Inner II. There are significant correlations between the ice phenology parameters and climatic factors in the Inner basin, which can pass a two-tailed test with a confidence level of 0.01 (Figure 8). It is probably because the climate factors differ with different lake surroundings (latitude, altitude, etc.) naturally (Guo et al. 2018).

The mean air temperature, LSWT and wind speed for each of the study lakes are calculated. For every 1℃ increase in air temperature or LSWT or 1 m s^{-1} increase in wind speed, the ice cover duration is shortened by 13.75 days, 18.87 days and 29.81 days, respectively (Table 5). LSWT has the highest correlation with lake ice phenology among the three climatic factors (Figure 8, Table 5) (Bussieres et al., 2002). In addition, climate variability and changes have greater effects on lake break-up dates than freeze-up dates (Figure 8, Table 5) (Palecki & Barry, 1986).

The energy available for water freeze-up in a lake is affected by the heat exchange with the atmosphere, heat stored in the water body, and inflows of water (Williams, 1965). The heat exchange with the atmosphere is mainly determined by climatic factors such as air/water temperature, wind and solar radiation, while heat storage in a lake is determined additionally by lake morphometry (Williams, 1965; Brown & Duguay, 2010), which will be discussed in the next section. The ice break-up is affected by heat gain from the atmosphere, solar radiation, snow and ice conditions, wind and currents, and inflows (Williams, 1965). Air and water temperature directly drives the lake heat balance and thus plays the main role in the ice cover regime (Kouraev et al., 2007), but the influence of wind is more complex. On the one hand, wind will bring cold or warm currents, which affect the water surface temperature, and on the other hand, the dynamic effects of wind could break the thin ice (Kouraev et al., 2007; Brown & Duguay, 2010). However, without detailed field observations, it is difficult to discuss the detailed effects of these climatic factors on lake ice phenology on the TP lakes.

5.2.2. Lake location, physico-chemical conditions and other factors

To control the differences in climate conditions, the correlations between lake ice phenology and lake altitude, area, and mineralization are calculated separately for the Inner I and Inner II. Some of these lakes have no historical records of mineralization; thus, only the salt lakes with mineralization data are used (Table 6).

There is a significant positive correlation between the altitudes and break-up end dates of the lakes in the Inner basin. The higher the altitude, the later the break-up end date and the longer the ice cover duration. There is an obvious autocorrelation between the altitude and climatic conditions that together affect the break-up time of the lakes, while the freeze-up time is mainly affected by the physical and chemical characteristics of the lakes (Adrian et al., 2009; Yao et al., 2016).

Lakes with larger areas have more water-storage capacity and a stronger dynamic effect, resulting in a longer freeze-up duration (Yao et al., 2016). Furthermore, wind can break up the initial ice cover more easily (Kouraev et al., 2007; Brown & Duguay, 2010). Lakes with long freeze-up durations in the Inner basin such as Qinghai Lake, Selin Co and Ngangla Ringco are all lakes with areas larger than 500 km^2 (Table A1). In theory, lakes with higher mineralizations should have a lower ice point, as well as a later freeze-up date, earlier break-up date and shorter ice cover duration (Yao et al., 2016). Lakes, such as Selin Co, Nam Co, and Tu Co, with large areas but low mineralization may affect the results of the correlation analysis (Table 6). In this case, lake size has a greater impact on the ice phenology than does the mineralization. At the same time, currently available mineralization records are from the 1970s to 1990s (Wang & Dou, 1998). In the context of climate change, the mineralization of lakes on the TP may have changed greatly over the past several decades. For example, the reduction of lake water volume may lead to an increase in mineralization and the expansion of the lake area may lead to a desalination of water.

Lexiewudan Co, which has the highest change rate of ice phonology over the 17 years, had a mineralization of 135.50 g L^{-1} in 1990 (Wang & Dou, 1998) and dropped to 89.47 g L^{-1} in 2010 (He et al., 2015). The lake came through an obvious process of desalination. Apart from this, the lake is recharged with ice-snow meltwater and large amounts of spring water (Wang & Dou, 1998). The special recharge form may also be one of the reasons that caused the large change in ice phenology. In addition, Dogaicoring Qangco may have similar reasons for the large changes in recent years, as the lake is nearby Lexiewudan Co and has similar conditions as Lexiewudan Co.

Shallow lakes require less heat to freeze-up and have earlier freeze-up dates (Kropacek et al., 2013; Yao et al., 2016). The physical characteristics determine the thermodynamics of a lake and sometimes have more of an impact on the ice phenology than do the chemical conditions. For example, the weather conditions of Gahai and Qinghai Lake are similar, and the freeze-up dates are nearly on the same day. As one of the remaining sub-lakes of Qinghai Lake, Gahai has no surface inflow and a smaller area (Gahai: 44.68 km^2, Qinghai Lake: 4,254.9 km^2, Wan et al., 2014) as well as a shallower depth (Gahai: 8.0~9.5 m, Qinghai Lake: average of 17.9 m, Wang & Dou, 1998). Although Gahai has a higher mineralization of 31.73 g L^{-1} than does Qinghai Lake (13.84 g L^{-1}) (Wang & Dou, 1998), the mean freeze-up start date is 15 days earlier than that of Qinghai Lake.

6. Conclusions

Approximately two-thirds of the cloud cover from the MODIS daily snow cover products can be eliminated by gap filling approach combining Terra and Aqua data and using the pixels within two days before and after the cloud covered pixel. The water cover classification from cloud-removed MODIS data agree well with the Landsat data (28 scenes, MAE = 4.58%) for two validated lakes (Nam Co and Selin Co) during the freeze-up and break-up periods. On this basis, the freeze-up start and break-up end dates of the 58 lakes on the TP from 2001 to 2017 are extracted. The freeze-up end and break-up start dates of 18 lakes were simultaneously extracted, and the lake ice durations (including freeze-up duration, complete freezing duration, break-up duration and ice cover duration) are calculated based on freeze-up/break-up dates. Compared to freeze-up dates (MAEs range from 2.92 to 7.25 days), the break-up dates (MAEs range from 1.75 to 3.25 days) have a better consistent with different passive microwave data sets (derived from AMSR-E/2 and SSM/I).

From late October to mid-January of the following year, the lakes on the TP begin to freeze one after another (mainly from northern part to southern part). Over 17 years, the freeze-up start dates of 81.03% of lakes have been delayed at a mean rate of 0.55 d yr^{-1}, and the other 18.97% of lakes have advancing freeze-up start date at a mean change rate of 0.44 d yr^{-1}. From late March to early July, the lakes gradually end their ice cover periods (mainly from southern part to northern part). Over 17 years, the lakes whose break-up end dates have been delayed and advanced account for 50% each, with mean change rates of 0.69 d yr^{-1} and 0.39 d yr^{-1}, respectively. The mean ice cover duration of 58 lakes is 157.78 days, of which the shortest is less than three months, and the longest is eight months. From 2001 to 2017, there are 18 lakes with ice cover durations that extended at a mean change rate of 1.11 d yr^{-1}, and 40 lakes shortened their ice cover durations at a mean change rate of 0.80 d yr^{-1}. Furthermore, the freeze-up and break-up processes of 18 lakes are extracted; the mean freeze-up duration is 9.81 days, the mean break-up duration is 13.01 days, and the mean complete freezing duration is 121.12 days. Most lakes have shorter freeze-up durations than break-up durations, and the freeze-up and break-up rates of most lakes have increased over the 17 years.

The ice phenology is influenced by climatic conditions, geographical location, and the physico-chemical characteristics of the lake. Lakes in the region with a lower altitude, higher air/water temperature and higher wind speed are inclined to have later freeze-up and earlier break-up dates, as well as shorter ice cover durations. The physico-chemical characteristics of the lakes mainly affect the freeze-up dates; deeper lakes with larger areas and higher mineralizations tend to have later freeze-up dates. Sometimes lake physical conditions may have a greater impact on ice phenology than do the chemical conditions.

The lack of historical observational data makes it difficult to study lake ice phenology on the TP without using remote sensing data. The quality of MODIS daily snow cover products limits the number of lakes that can be studied, and the low spatial resolution of reanalysis data makes it difficult to represent the actual meteorological conditions of each lake. It is also difficult to ensure the reliability of historical lake physico-chemical data that were collected several decades ago. With the improvement of data and methods, lake ice phenology on the TP and its influencing factors can hopefully be further analyzed in the future. In addition, further research is required on the comparisons of lake ice phenology characteristics derived from different sources of remote sensing data and different retrieval methods, as well as in different climatic regions.

Acknowledgments

This work is supported financially by the Program for National Natural Science Foundation of China (No. 41830105) and also funded by the International Scholar Exchange Fellowship (ISEF) program at KFAS (Korean Foundation of Advanced Studies). The MODIS snow data used in this study are obtained from the National Snow and Ice Data Center (http://nsidc.org). The Landsat data used are obtained from the Google Earth Engine platform (https://earthengine.google.com/). The Reanalysis data are from the National Oceanic and Atmospheric Administration (https://www.esrl.noaa.gov/). We would thank the two anonymous reviewers and editors for valuable comments and suggestions to greatly improve the paper.

References

Adrian, R., O'Reilly, C. M., Zagarese, H., Baines, S. B., Hessen, D. O., Keller, W., et al. (2009). Lakes as sentinels of climate change. *Limnology and Oceanography*, 54(6), 2283-2297. http://dx.doi.org/10.4319/lo.2009.54.6_part_2.2283.

Brown, L. C. & Duguay, C. R. (2010). The response and role of ice cover in lake-climate interactions. *Progress in Physical Geography*, 34, 671-704. http://dx.doi.org/10.1177/0309133310375653.

Bussieres, N., Verseghy, D. & MacPherson, J. I. (2002). The evolution of AVHRR-derived water temperatures over boreal lakes. *Remote sensing of environment*, 80(3), 373-384. https://doi.org/10.1016/S0034-4257(01)00317-0.

Cai, Y., Ke, C. Q. & Duan, Z. (2017). Monitoring ice variations in Qinghai Lake from 1979 to 2016 using passive microwave remote sensing data. *Science of the Total Environment*, 607-608, 120-131. http://dx.doi.org/10.1016/j.scitotenv.2017.07.027.

Chaouch, N., Temimi, M., Romanov, P., Cabrera, R., McKillop, G. & Khanbilvardi, R. (2014). An automated algorithm for river ice monitoring over the Susquehanna River using the MODIS data. *Hydrological Processes*, 28(1), 62-73. http://dx.doi.org/10.1002/hyp.9548.

Che, T., Li, X. & Jin, R. (2009). Monitoring the frozen duration of Qinghai Lake using satellite passive microwave remote sensing low frequency data (in Chinese). *Chinese Science Bulletin*, 54(6), 787-791. http://dx.doi.org/10.1007/s11434-009-0044-3.

Dörnhöfer, K. & Oppelt, N. (2016). Remote sensing for lake research and monitoring-Recent advances. *Ecological Indicators*, 64, 105-122. http://dx.doi.org/10.1016/j.ecolind.2015.12.009.

Du, J. Y., Kimball, J. S., Duguay, C., Kin, Y. & Watts, J. D. (2017). Satellite microwave assessment of Northern Hemisphere lake ice phenology from 2002 to 2015. *The Cryosphere*, 11, 47-63. http://dx.doi.org/10.5194/tc-2016-199.

Duguay, C. R., Bernier, M., Gauthier, Y. & Kouraev, A. (2015). Remote sensing of lake and river ice. In M. Tedesco (Ed.) *Remote Sensing of the Cryosphere* (pp. 273-306). Oxford, UK: Wiley-Blackwell. http://dx.doi.org/10.1002/9781118368909.ch12.

Duguay, C. R. & Lafleur, P. M. (2003). Estimating depth and ice thickness of shallow subarctic lakes using spaceborne optical and SAR data. *International Journal of Remote Sensing*, 24(3), 475–489. http://dx.doi.org/10.1080/01431160304992.

Duguay, C. R., Pultz, T. J., Lafleur, P. M. & Drai, D. (2002). RADARSAT backscatter characteristics of ice growing on shallow sub-arctic lakes, Churchill, Manitoba, Canada. *Hydrological Processes*, 16(8), 1631–1644. http://dx.doi.org/10.1002/hyp.1026.

Gafurov, A. & Bárdossy, A. (2009). Cloud removal methodology from MODIS snow cover product. *Hydrology and Earth System Sciences*, 13(7), 1361-1373. http://dx.doi.org/10.5194/hess-13-1361-2009.

Gao, Y., Xie, H. J., Lu, N., Yao, T. D. & Liang, T. G. (2010). Toward advanced daily cloud-free snow cover and snow water equivalent products from Terra–Aqua MODIS and Aqua AMSR-E measurements. *Journal of Hydrology*, 385(1-4), 23-35. https://doi.org/10.1016/j.jhydrol.2010.01.022.

Gao, Y., Xie, H. J., Yao, T. D. & Xue, C. S. (2010). Integrated assessment on multi-temporal and multi-sensor combinations for reducing cloud obscuration of MODIS snow cover products of the Pacific Northwest USA. *Remote Sensing of Environment*, 114(8), 1662-1675. https://doi.org/10.1016/j.rse.2010.02.017.

Geldsetzer, T., Sanden, J. V. D. & Brisco, B. (2010). Monitoring lake ice during spring melt using RADARSAT-2 SAR. *Canadian Journal of Remote Sensing*, 36(S2), S391-S400.

Guo, L. N., Wu, Y. H., Zheng, H. X., Zhang, B., Li, J. S., Zhang, F. F. & Shen, Q. (2018). Uncertainty and variation of remotely sensed lake ice phenology across the Tibetan Plateau. *Remote Sensing*, 10, 1534. https://doi.org/10.3390/rs10101534.

Hall, D. K. & Riggs, G. A. (2007). Accuracy assessment of the MODIS snow products. *Hydrological Processes*, 21(12), 1534-1547. http://dx.doi.org/10.1002/hyp.6715.

Hall, D. K., Riggs, G. A. & Salomonson, V. V. (2001). Algorithm Theoretical Basis Document (ATBD) for the MODIS Snow and Sea Ice-Mapping Algorithms. https://modis-snow-ice.gsfc.nasa.gov/?c=atbd&t=atbd.

He, L., Han, F. Q., Han, W. X., Yan, J. P., Li, B. K., Han, Y. Z., et al. (2015). Hydrochemical Characteristics of Lexiewudan Lake in Hoh Xil, Qinghai (in Chinese). *Journal of Salt Lake Research*, 23(2), 28-33.

Howell, S. E. L., Brown, L. C., Kang, K. -K. & Duguay, C. R. (2009). Variability in ice phenology on Great Bear Lake and Great Slave Lake, Northwest Territories, Canada, from SeaWinds/QuikSCAT: 2000-2006. *Remote Sensing of Environment*, 113(4), 816-834. http://dx.doi.org/10.1016/j.rse.2008.12.007.

Huang, H., Liang, T., Zhang, X. & Guo, Z. (2011). Validation of MODIS snow cover products using Landsat and ground measurements during the 2001-2005 snow seasons over northern Xinjiang, China. *International Journal of Remote Sensing*, 32(1), 133-152. http://dx.doi.org/10.1080/01431160903439924.

Jeffries, M. O., Morris, K., Weeks, W. F. & Wakabayashi, H. (1994). Structural and stratigraphic features and ERS 1 synthetic aperture radar backscatter characteristics of ice growing on shallow lakes in NW Alaska, winter 1991–1992. *Journal of Geophysical Research Oceans*, 99(C11), 22459–22471. http://dx.doi.org/10.1029/94JC01479.

Kang, S. C., Xu, Y. W., You, Q. L., Flügel, W. -A., Pepin, N. & Yao, T. D. (2010). Review of climate and cryospheric change in the Tibetan Plateau. *Environmental Research Letters*, 5, 015101. http://dx.doi.org/10.1088/1748-9326/5/1/015101.

Ke, C. Q., Tao, A. Q. & Jin, X. (2013). Variability in the ice phenology of Nam Co Lake in central Tibet from scanning multichannel microwave radiometer and special sensor microwave/imager: 1978 to 2013. *Journal of Applied Remote Sensing*, 7, 073477. http://dx.doi.org/10.1117/1.JRS.7.073477.

Kendall, M. G. (1975). *Rank Correlation Methods*. London: Charles Griffin.

Kouraev, A. V., Semovski, S. V., Shimaraev, M. N., Mognard, N. M., Legrésy, B & Rémy, F. (2007). The ice regime of Lake Baikal from historical and satellite data: Relationship to air temperature, dynamical, and other factors. *Limnology and Oceanography*, 52(3), 1268-1286. http://dx.doi.org/10.4319/lo.2007.52.3.1268.

Kropáček, J., Maussion, F., Chen, F., Hoerz, S. & Hochschild, V. (2013). Analysis of ice phenology of lakes on the Tibetan Plateau from MODIS data. *The Cryosphere*, 7(1), 287-301. http://dx.doi.org/10.5194/tc-7-287-2013.

Latifovic, R. & Pouliot, D. (2007). Analysis of climate change impacts on lake ice phenology in Canada using the historical satellite data record. *Remote Sensing of Environment*, 106(4), 492-507. http://dx.doi.org/10.1016/j.rse.2006.09.015.

Liang, T. G., Zhang, X. T., Xie, H. J., Wu, C. X., Feng, Q. S., Huang, X. D. & Chen, Q. G. (2008). Toward improved daily snow cover mapping with advanced combination of MODIS and AMSR-E measurements. *Remote Sensing of Environment*, 112(10), 3750-3761. https://doi.org/10.1016/j.rse.2008.05.010.

Liu, X. D. & Chen, B. D. (2000). Climatic warming in the Tibetan Plateau during recent decades. *International Journal of Climatology*, 20, 1729-1742. http://dx.doi.org/10.1002/1097-0088(20001130)20:14<1729::AID-JOC556>3.0.CO;2-Y.

López-Burgos, V., Gupta, H. V. & Clark, M. (2013). Reducing cloud obscuration of MODIS snow cover area products by combining spatio-temporal techniques with a probability of snow approach. *Hydrology and Earth System Sciences*, 17(5), 1809-1823. http://dx.doi.org/10.5194/hess-17-1809-2013.

Mann, H. B. (1945). Non-parametric tests against trend. *Econometrica*, 13, 245-259. http://dx.doi.org/10.2307/1907187.

Maurer, E. P., Rhoads, J. D., Dubayah, R. O. & Lettenmaier, D. P. (2003). Evaluation of the snow-covered area data product from MODIS. *Hydrological Processes*, 17, 59-71. http://dx.doi.org/10.1002/hyp.1193.

Morris, K., Jeffries, M. O. & Weeks, W. F. (1995). Ice processes and growth history on Arctic and sub-Arctic lakes using ERS-1 SAR data. *Polar Record*, 31(177), 115–128. http://dx.doi.org/10.1017/S0032247400013619.

Palecki, M. A. & Barry, R. G. (1986). Freeze-up and break-up of lakes as an index of temperature changes during the transition seasons: a case study for Finland. *Journal of Climate and Applied Climatology*, 25, 893-902. https://doi.org/10.1175/1520-0450(1986)025<0893:FUABUO>2.0.CO;2.

Parajka, J. & Blöschl, G. (2008). The value of MODIS snow cover data in validating and calibrating conceptual hydrologic models. *Journal of Hydrology*, 358(3-4), 240-258. http://dx.doi.org/10.1016/j.jhydrol.2008.06.006.

Paudel, K. P. & Andersen, P. (2011). Monitoring snow cover variability in an agropastoral area in the Trans Himalayan region of Nepal using MODIS data with improved cloud removal methodology. *Remote Sensing of Environment*, 115(5), 1234-1246. http://dx.doi.org/10.1016/j.rse.2011.01.006.

Qiu, J. (2008). The Third Pole. *Nature*, 454(7203), 393-396. http://dx.doi.org/10.1038/454393a.

Reed, B., Buddle, M., Spencer, P. & Miller, A. E. (2009). Integration of MODIS-derived metrics to assess interannual variability in snowpack, lake ice, and NDVI in southwest Alaska. *Remote Sensing of Environment*, 113(7), 1443-1452. http://dx.doi.org/10.1016/j.rse.2008.07.020.

Rouse, W. R., Oswald, C. J., Binyamin, J., Spence, C., Schertzer, W. M., Blanken, P. D., et al. (2005). The Role of Northern Lakes in a Regional Energy Balance. *Journal of Hydrometeorology*, 6, 291-305. https://doi.org/10.1175/JHM421.1.

Sorman, A. U., Akyurek, Z., Sensoy, A., Sorman, A. A. & Tekeli, A. E. (2007). Commentary on comparison of MODIS snow cover and albedo products with ground observations over the mountainous terrain of Turkey. *Hydrology and Earth System Sciences*, 11(4), 1353-1360. http://dx.doi.org/10.5194/hess-11-1353-2007.

Wan, W., Li, H., Xie, H. J., Hong, Y., Long. D., Zhao, L. M., et al. (2017). A comprehensive data set of lake surface water temperature over the Tibetan Plateau derived from MODIS LST products 2001–2015. *Scientific Data*, 4, 170095. http://dx.doi.org/10.1038/sdata.2017.95.

Wan, W, Xiao, P. F., Feng, X. Z., Li, H., Ma, R. H., Duan, H. T. & Zhao, L. M. (2014). Monitoring lake changes of Qinghai-Tibetan Plateau over the past 30 years using satellite remote sensing data. *Chinese Science Bulletin*, 59(10), 1021-1035. http://dx.doi.org/10.1007/s11434-014-0128-6.

Wang, S. M. & Dou, H. S. (1998). *Records of Chinese Lakes* (in Chinese). Beijing, CHN: Science Press.

Weber, H., Riffler, M., Nõges, T. & Wunderle, S. (2016). Lake ice phenology from AVHRR data for European lakes: An automated two-step extraction method. *Remote Sensing of Environment*, 174, 329-340. http://dx.doi.org/10.1016/j.rse.2015.12.014.

Wei, Q. F. & Ye, Q. H. (2010). Review of lake ice monitoring by remote sensing (in Chinese). *Progress in Geography*, 29(7), 803–810.

Williams, G. P. (1965). Correlating freeze-up and break-up with weather conditions. *Canadian Geotechnical Journal*, 11(4), 313-326. http://doi.org/10.1139/t65-047.

Yao, X. J., Li, L., Zhao, J., Sun, M. P., Li, J., Gong, P. & An, L. N. (2016). Spatial-temporal variations of lake ice phenology in the Hoh Xil region from 2000 to 2011. *Journal of Geographical Sciences*, 26(1), 70-82. http://dx.doi.org/10.1007/s11442-016-1255-6.

Yu, J. Y., Zhang, G. Q., Yao, T. D., Xie, H. J., Zhang, H. B., Ke, C. Q. & Yao, R. Z. (2016). Developing Daily Cloud-Free Snow Composite Products from MODIS Terra–Aqua and IMS for the Tibetan Plateau. *IEEE Transactions on Geoscience & Remote Sensing*, 54(4), 2171-2180. http://doi.org/10.1109/TGRS.2015.2496950.

Zhang, G. Q., Yao, T. D., Xie, H. J., Kang, S. C. & Lei, Y. B. (2013). Increased mass over the Tibetan Plateau: From lakes or glaciers? *Geophysical Research Letters*, 40(10), 2125-2130. http://dx.doi.org/10.1002/grl.50462.

Zhang, G. Q., Yao, T. D., Xie, H. J., Qin, J., Ye, Q. H., Dai, Y. F. & Guo, R. F. (2014). Estimating surface temperature changes of lakes in the Tibetan Plateau using MODIS LST data. *Journal of Geophysical Research Atmospheres*, 119(14), 8552–8567. http://dx.doi.org/10.1002/2014JD021615.

Zhang, G. Q., Yao, T. D., Xie, H. J., Zhang, K. X. & Zhu, F. J. (2014). Lakes' state and abundance across the Tibetan Plateau. *Chinese Science Bulletin*, 59(24), 3010-3021. http://dx.doi.org/10.1007/s11434-014-0258-x.

Figure Captions

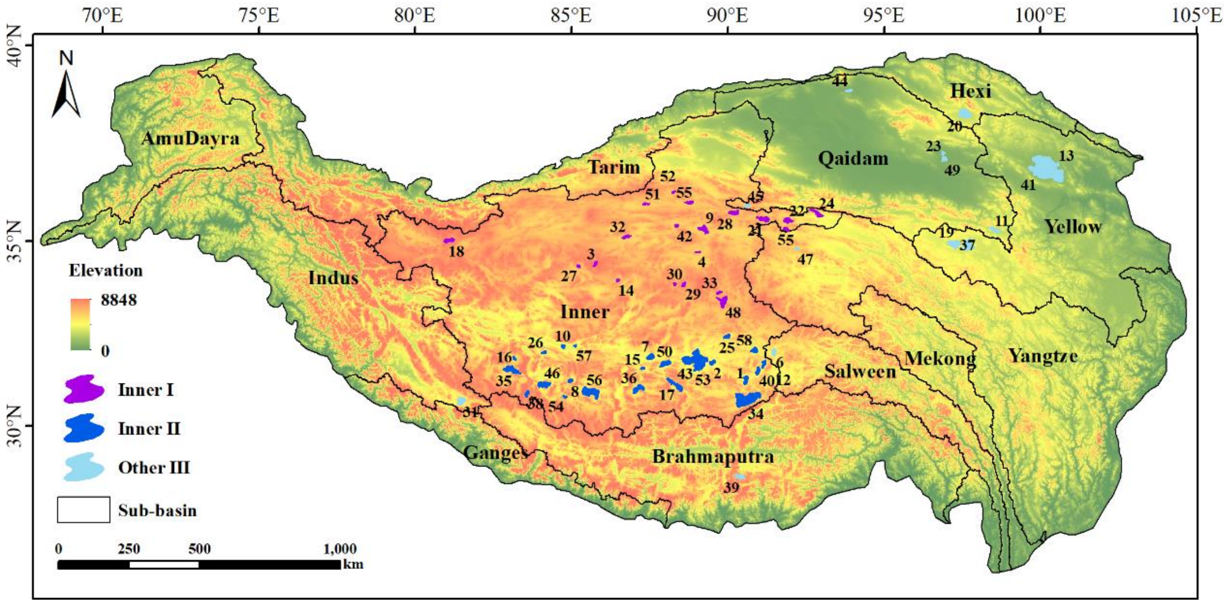

Figure 1. Locations of the TP and its sub-basins. 58 study lakes are grouped into three sub-areas labeled Inner I, Inner II, and Other III (The lake names are listed in Table A1 in Appendix A).

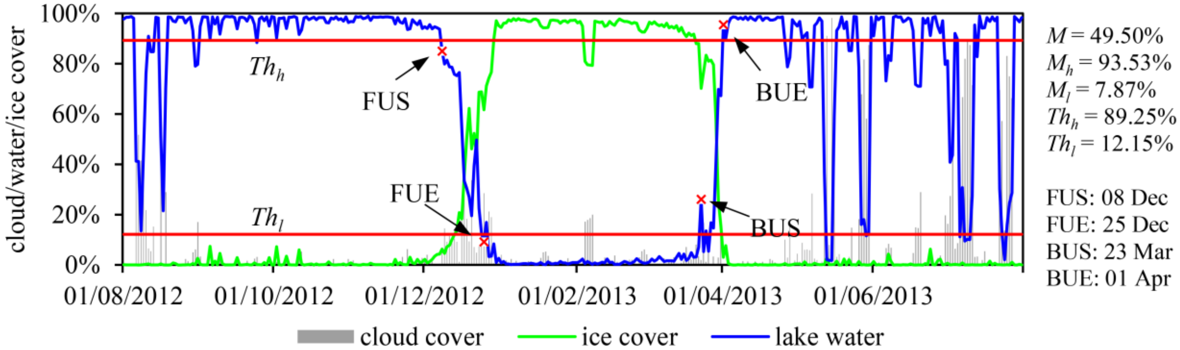

Figure 2. The extraction of the freeze-up/break-up dates in Qinghai Lake during 2013. Two red lines represent the two thresholds for extracting freeze-up/break-up dates, and four red stars, from left to right, represent the freeze-up start (FUS), freeze-up end (FUE), break-up start (BUS), and break-up end (BUE) dates.

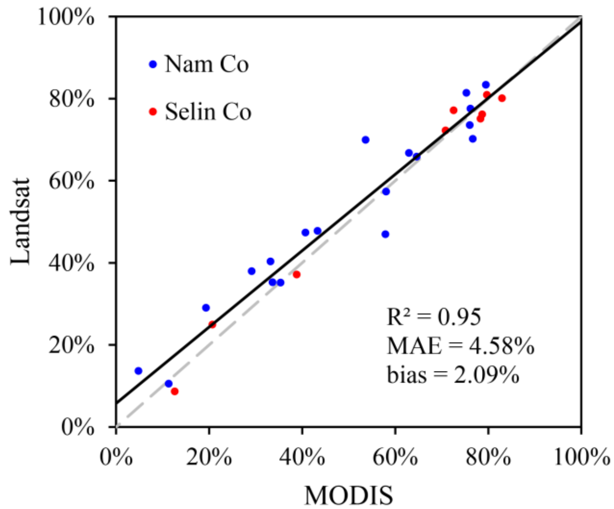

Figure 3. Comparison of lake water cover proportions during freeze-up/break-up periods derived from the MODIS cloud-removed data and Landsat data.

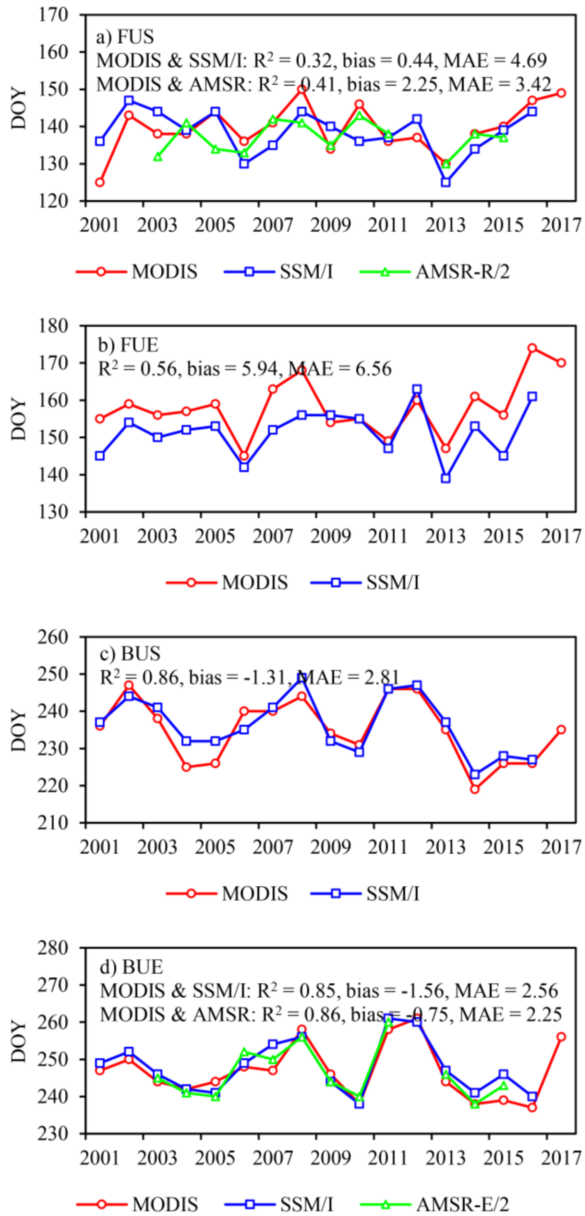
a) FUS
MODIS & SSM/I: R² = 0.32, bias = 0.44, MAE = 4.69
MODIS & AMSR: R² = 0.41, bias = 2.25, MAE = 3.42
DOY
MODIS
SSM/I
AMSR-R/2
b) FUE
R² = 0.56, bias = 5.94, MAE = 6.56
DOY
MODIS
SSM/I
c) BUS
R² = 0.86, bias = -1.31, MAE = 2.81
DOY
MODIS
SSM/I
d) BUE
MODIS & SSM/I: R² = 0.85, bias = -1.56, MAE = 2.56
MODIS & AMSR: R² = 0.86, bias = -0.75, MAE = 2.25
DOY
MODIS
SSM/I
AMSR-E/2
2001 2003 2005 2007 2009 2011 2013 2015 2017

Figure 4. Comparisons of ice phenology for Qinghai Lake derived from MODIS data and passive microwave data. **a**. Comparisons between freeze-up start (FUS) dates derived from MODIS, SSM/I and AMSR; **b**. comparisons between freeze-up end (FUE) dates derived from MODIS and SSM/I; **c**. comparisons between break-up start (BUS) dates derived from MODIS and SSM/I; and **d**. comparisons between break-up end (BUE) dates derived from MODIS, SSM/I and AMSR. DOY means the day of the year relative to 1 August.

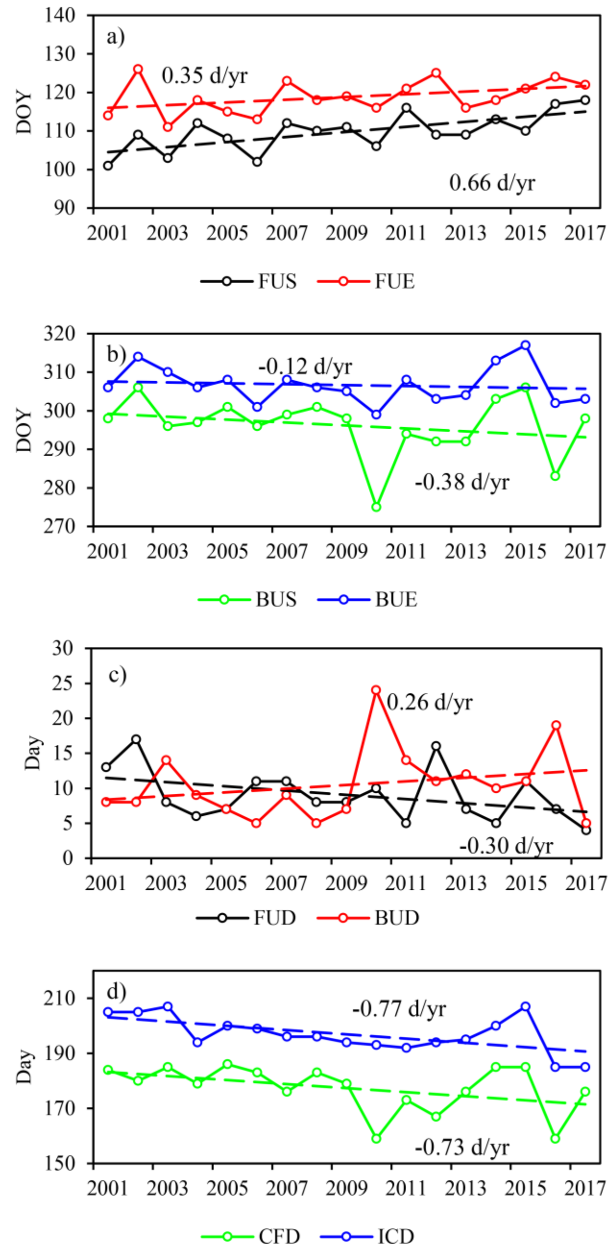

Figure 5. The ice phenology and its trend for Har Lake from 2001 to 2017. **a**. Freeze-up dates and their trends; **b**. break-up dates and their trends; **c**. freeze-up duration and break-up duration and their trends; and **d**. complete freezing durations and ice cover duration and their trends over 17 years. (FUS: freeze-up start, FUE: freeze-up end, BUS: break-up start, BUE: break-up end,

FUD: freeze-up duration, BUD: break-up duration, CFD: complete freezing duration, and ICD: ice cover duration)

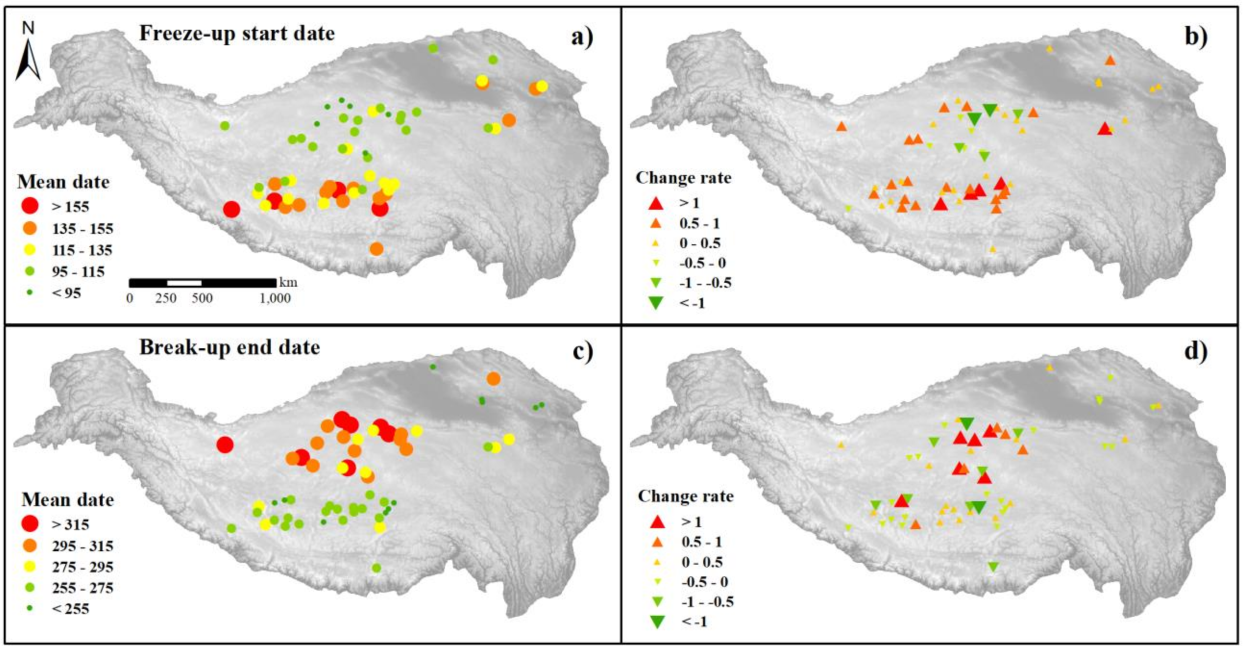

Figure 6. Mean and change rate (d yr^{-1}) of freeze-up start and break-up end dates of the 58 lakes from 2001 to 2017. **a**. Mean freeze-up start date; **b**. change rate of freeze-up start date; **c**. the mean break-up end date; and **d**. change rate of break-up end date. (The freeze-up/break-up dates are DOYs.)

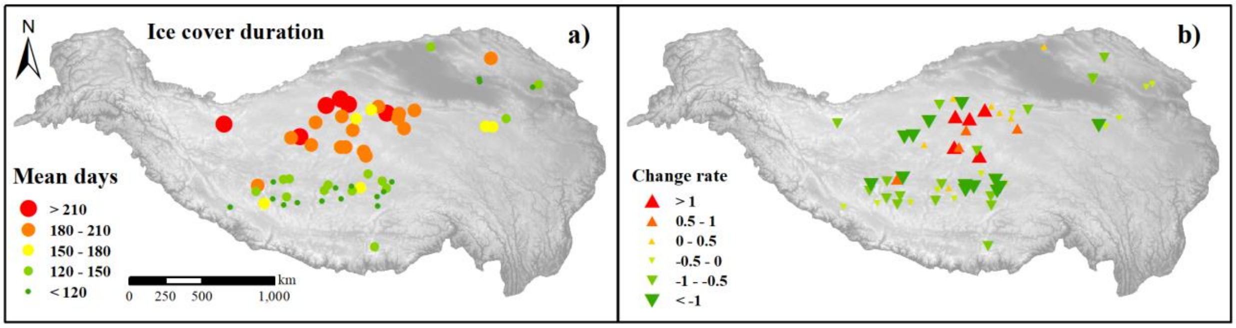

Figure 7. Mean and change rate of ice cover duration for the 58 lakes from 2001 to 2017. **a**. Mean ice cover duration; and **b**. change rate of ice cover duration.

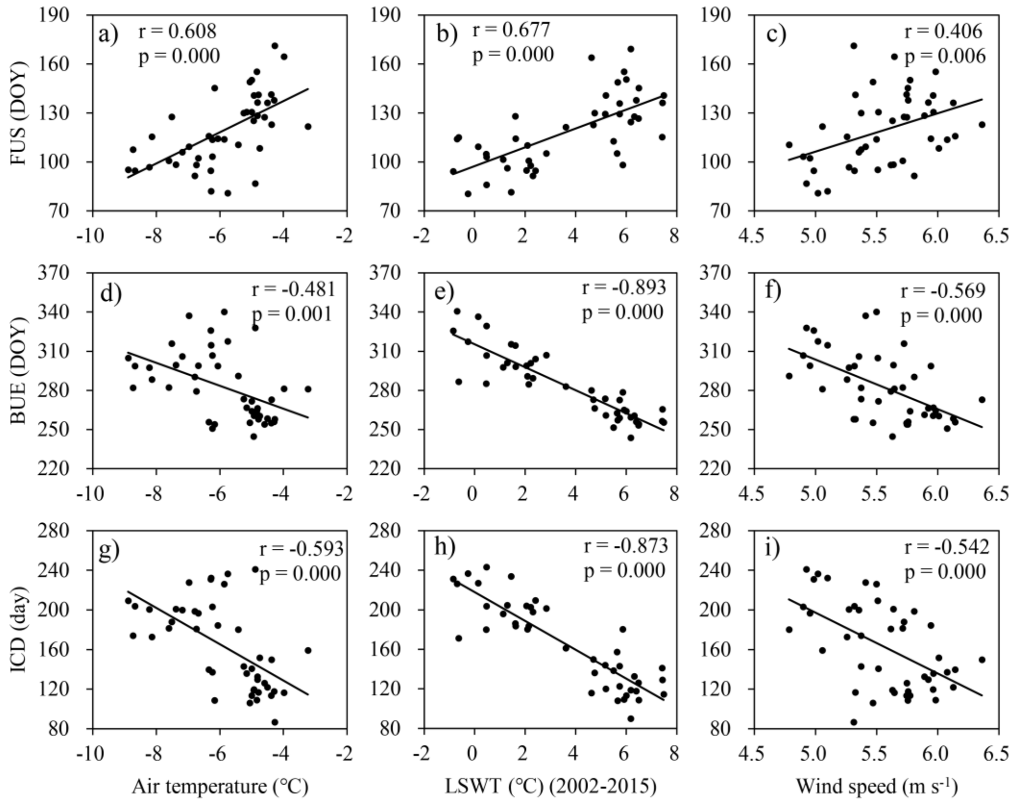

Figure 8. Correlations between mean air temperature, LSWT (lake water surface temperature), wind speed and mean lake ice phenology parameters in the Inner basin from 2001 to 2017. (FUS: freeze-up start, BUE: break-up end and ICD: ice cover duration)

Table Captions

Table 1. *Comparison of Cloud Cover for 58 Lakes During 2013, With and Without Cloud Removal*

	Mean	Maximum	Minimum
Original Terra	44.97%	63.98% (Taiyang Lake)	30.07% (Zhaxi Co)
Original Aqua	51.70%	69.43% (Taiyang Lake)	31.47% (Mapam Yumco)
Combined T&A	31.02%	50.94% (Taiyang Lake)	18.58% (Lagkor Co)
Cloud removal	16.54%	35.49% (Taiyang Lake)	4.52% (Zhari Namco)

Table 2. *Summary of the Comparison Results for Freeze-up Start (FUS) and Break-up End (BUE) Dates Derived From MODIS Snow Products, AMSR-E/2 Data Sets and SSM/I Data Sets*

		FUS			BUE		
	Lake	R^2	bias	MAE	R^2	bias	MAE
MODIS compared against AMSR-E/2	Gyaring Lake	0.09	0.50	5.33	0.97	0.67	2.50
	Har Lake	0.62	-0.58	2.92	0.84	-0.83	2.17
	Nam Co	0.19	3.58	7.08	0.79	0.75	3.25
	Ngangla Ringco	0.28	-4.33	5.83	0.91	-0.17	1.83
	Ngoring Lake	0.19	0.83	6.83	0.93	-0.58	2.25
	Qinghai Lake	0.41	2.25	3.42	0.86	-0.75	2.25
	Selin Co	0.48	-7.25	7.25	0.93	0.75	1.75
	Zhari Namco	0.54	-2.83	3.83	0.96	-1.50	2.00
	Average	0.35	-0.98	5.31	0.90	-0.21	2.25
MODIS compared against SSM/I	Nam Co	0.42	-5.38	6.92	0.35	0.00	6.31
	Qinghai Lake	0.32	0.44	4.69	0.85	-1.56	2.56
	Average	0.37	-2.47	5.81	0.60	-0.78	4.44

Table 3. *The Number and Percentage of Lakes, Their Mean Date/Days and Change Rates (d yr^{-1}) Within Three Sub-areas: Inner I, Inner II and Other III (FUS: Freeze-up Start, BUE: Break-up End, and ICD: Ice Cover Duration)*

		Inner I	Inner II	Other III	All lakes
FUS	Mean (all)	20 (34.48%), 10 Nov	24 (41.38%), 13 Dec	14 (24.14%), 5 Dec	58 (100%), 30 Nov
	Delaying	10 (50.00%), 0.57	24 (100.00%), 0.64	13 (92.86%), 0.35	47 (81.03%), 0.55
	Advancing	10 (50.00%), -0.49	0	1 (7.14%), -0.00	11 (18.97%), -0.44
BUE	Mean (all)	3 Jun	20 Apr	26 Apr	6 May
	Delaying	12 (60.00%), 1.21	11 (45.83%), 0.32	6 (42.86%), 0.35	29 (50.00%), 0.69
	Advancing	8 (40.00%), -0.51	13 (54.17%), -0.44	8 (57.14%), -0.19	29 (50.00%), -0.39
ICD	Mean (all)	204.46	128.21	141.79	157.78
	Extending	11 (55.00%), 1.62	3 (12.50%), 0.41	4 (28.57%), 0.24	18 (31.03%), 1.11
	Shortening	9 (45.00%), -0.92	21 (87.50%), -0.89	10 (71.43%), -0.50	40 (68.97%), -0.80

Table 4. *Comparison of Climate Conditions Between the Inner I and Inner II From 2001 to 2017 (CR: Change Rates, LSWT: Lake Water Surface Temperature)*

	Air temperature		LSWT (2002-2015)		Wind speed	
	Mean (°C)	CR (0.01 °C yr^{-1})	Mean (°C)	CR (0.01 °C yr^{-1})	Mean (m s^{-1})	CR (0.01 m s^{-1} yr^{-1})
Inner I	-6.98	4.30	1.10	-5.26	5.32	1.07
Inner II	-4.94	6.89	5.48	-1.47	5.76	2.31

Table 5. *The Number of Lakes Whose Ice Phenology Has a Significant Correlation ($p < 0.05$) With Climatic Factors, and the Mean Change Rates (FUS: Freeze-up Start, BUE: Break-up End, and ICD: Ice Cover Duration, LSWT: Lake Water Surface Temperature)*

	Air temperature (d $°C^{-1}$)	LSWT (d $°C^{-1}$)	Wind speed (d m^{-1} s)
FUS	7, 8.53	9, 2.55	7, 13.89
BUE	10, -11.11	30, -14.56	11, -26.83
ICD	17, -13.75	23, -18.87	16, -29.81

Table 6. *Correlations Between Ice Phenology and the Physical Attributes of the Lakes in the Inner I and Inner II (FUS: Freeze-up Start, BUE: Break-up End, and ICD: Ice Cover Duration)*

	Inner I			Inner II		
	Altitude	Area	Mineralization[a]	Altitude	Area	Mineralization[b]
FUS	0.24	0.44	-0.04	-0.03	0.48*	-0.17
BUE	0.52*	-0.03	-0.28	0.65**	0.18	-0.03
ICD	0.28	-0.26	-0.24	0.34	-0.32	0.15

Note. [a] Calculated from eleven salt lakes. [b] Calculated from 19 salt lakes, and mineralization data are from Wang and Dou (1998). * Statistical significance at the 0.05 level. ** Statistical significance at the 0.01 level.

Appendix A

Table A1. *Lake Ice Phenology Statistics and the Change Rates (CR, d yr^{-1}) and Lake Characteristics for 58 Lakes From 2001 to 2017 (FUS: Freeze-up Start, FUE: Freeze-up End, BUS: Break-up Start, BUE: Break-up End, FUD: Freeze-up Duration, BUD: Break-up Duration, CFD: Complete Freezing Duration, and ICD: Ice Cover Duration)*

No.	Lake	Area (km^2)[a]	Altitude (m)[b]	Mean FUS	CR	Mean FUE	CR	Mean BUS	CR	Mean BUE	CR	Mean FUD	CR	Mean CFD	CR	Mean BUD	CR	Mean ICD	CR	Spatial location
1	Bamco	236.16	4560	16 Dec	0.82*					13 Apr	0.25							117.88	-0.56	I
2	Bangkog Co	136.34	4527	17 Nov	1.10*					18 Apr	-1.63**							151.82	-2.73**	I
3	Burog Co	89.91	5166	18 Nov	0.88**					4 Jul	-0.39							227.82	-1.26	I
4	Changhu Lake	49.98	4839	4 Nov	-0.24					1 Jun	0.28							209.29	0.52	I
5	Cuoda Rima	84.6	4783	11 Nov	0.13					26 May	0.42							196.59	0.29	III
6	Cuona Lake	188.54	4585	3 Dec	0.19					25 Mar	0.36							112.06	0.16	I
7	Dagze Co	269.07	4465	15 Dec	0.79**	20 Dec	0.63*	2 Apr	0.82	16 Apr	0.20	5.18	-0.16	103.59	0.19	13.35	-0.63**	122.12	-0.59	I
8	Dawa Co	110.55	4623	9 Dec	0.85*	14 Dec	0.71*	12 Apr	0.07	29 Apr	0.00	4.94	-0.14	118.65	-0.64*	17.29	-0.07	140.88	-0.85	I
9	Dogaicoring Qangco	313.68	4787	16 Nov	-1.12					9 May	3.50*							174.24	4.62	I
10	Dong Co	92.47	4394	22 Nov	0.27	28 Nov	0.20	1 Apr	1.10	8 Apr	1.02	6.18	-0.07	123.65	0.90	7.29	-0.08	137.12	0.75	I
11	Donggei Cuona Lake	230.65	4081	15 Dec	0.23*					10 May	0.21							145.53	-0.02	III
12	Dung Co	149.6	4551	6 Dec	0.77**					11 Apr	-0.35							126.29	-1.12	I
13	Gahai	44.68	3197	3 Dec	0.38					4 Apr	0.01							121.29	-0.37	III
14	Garkung Caka	59.33	4909	7 Nov	-0.04					27 May	0.13							200.82	0.17	I
15	Gemang Co	60.06	4605	15 Dec	0.35					24 Apr	0.05							129.76	-0.30	I
16	Gopug Co	59.68	4718	7 Nov	0.15					7 May	-0.88							181.00	-1.03	I
17	Goren Co	477.98	4649	29 Dec	0.25					21 Apr	0.25							113.59	0.00	I
18	Gozha Co	315.51	5080	22 Nov	0.67**					7 Jul	0.03							226.12	-0.64	II
19	Gyaring Lake	526.62	4290	16 Nov	1.02*					18 Apr	-0.27							153.12	-1.29	IV
20	Har Lake	596.39	4076	18 Nov	0.66**	27 Nov	0.35	24 May	-0.38	3 Jun	-0.12	9.06	-0.30	177.35	-0.73*	10.47	0.26	196.88	-0.77*	III
21	Hoh Xil Lake	315.95	4886	3 Nov	0.47	15 Nov	0.15	12 Jun	0.93*	22 Jun	0.58	11.47	-0.33	209.65	0.79	9.88*	-0.35	231.00	0.11	III

22	Huolunuo'er	259.24	4753	12 Nov	-0.64					3 Jun	-0.65							203.35	-0.01	III
23	Keluke Lake	54	2814	27 Nov	0.14					27 Mar	-0.40							119.35	-0.54	III
24	Kusai Lake	271.08	4475	19 Nov	0.80**	4 Dec	0.51*	6 May	0.09	18 May	-0.10	14.65	-0.28	153.71	-0.42	11.94	-0.19	180.29	-0.90*	III
25	Kyebxang Co	170.98	4615	1 Dec	0.48	9 Dec	0.42*	17 Apr	0.51	30 Apr	-0.01	7.59	-0.06	128.71	0.10	13.65	-0.52	149.94	-0.48	I
26	Lagkor Co	93.39	4467	24 Dec	0.80**	28 Dec	0.86**	30 Mar	-0.27	11 Apr	0.00	3.94	0.06	92.65	-1.13*	12.00	0.26	108.59	-0.81	I
27	Laxiong Co	60.75	4885	15 Nov	0.62**					2 Jun	-0.38							199.88	-1.01	I
28	Lexiewudan Co	247.58	4870	24 Nov	-1.22**					16 May	4.25**							172.76	5.46**	III
29	Lingguo Co	108.14	5062	6 Dec	-0.19					12 Jun	0.63							188.06	0.82	I
30	Longwei Co	52.88	4942	9 Nov	-0.52					10 May	1.40							181.41	1.93	I
31	Mapam Yumco	409.9	4585	13 Jan	0.00	22 Jan	0.04	20 Apr	0.13	29 Apr	-0.08	9.60	0.02	87.86	0.09	8.61	0.00	106.06	-0.08	II
32	Margai Caka	145.17	4793	3 Nov	0.50**					26 May	-0.64							203.82	-1.15*	I
33	Meiriqiecuomari	86	4947	31 Oct	-0.01					18 May	-0.58							198.65	-0.57	I
34	Nam Co	2040.9	4724	12 Jan	0.51					9 May	-0.21							116.59	-0.72	I
35	Ngangla Ringco	542.89	4716	9 Dec	0.75*	27 Dec	0.51*	14 Apr	0.30	1 May	0.10	18.76	-0.24	107.76	-0.21*	16.65	-0.20	143.18	-0.65	I
36	Ngangze Co	445.48	4685	4 Dec	1.25**	11 Dec	1.04	18 Mar	1.42	2 Apr	0.42	7.43	-0.15	96.50	0.38	15.18	-0.80	119.12	-0.82	I
37	Ngoring Lake	629.75	4267	1 Dec	0.25					8 May	-0.02							158.00	-0.27	IV
38	Palung Co	144.65	5101	30 Nov	0.18	8 Dec	0.31	20 Apr	-0.34	8 May	-0.20	7.94	0.12	132.47	-0.65	18.65	0.14	159.06	-0.38	I
39	Puma Yumco	294.11	5013	1 Jan	0.41					1 May	-0.54							120.24	-0.95	I
40	Pung Co	172.11	4529	20 Dec	0.75**					12 Apr	-0.29							113.59	-1.05	I
41	Qinghai Lake	4254.9	3194	18 Dec	0.40	6 Jan	0.49	23 Mar	-0.50	4 Apr	-0.07	18.59	0.09	76.82	-0.99**	11.94	0.43	107.35	-0.47	IV
42	Rola Co	82.52	4815	5 Nov	-0.36					25 May	1.24							200.59	1.60	I
43	Selin Co	2129.02	4539	19 Dec	0.71*	5 Jan	0.55	4 Apr	0.15	18 Apr	-0.56	16.29	-0.17	89.71	-0.39	13.76	-0.71**	119.76	-1.27*	I
44	Sugan Lake	101.4	2793	18 Nov	0.10	29 Nov	0.51	28 Mar	0.33	10 Apr	0.13	10.59	0.41	119.12	-0.19*	13.59	-0.20	143.29	0.02	III
45	Taiyang Lake	101.82	4881	22 Nov	0.46*					18 Jun	0.56							207.65	0.10	III
46	Taro Co	486.62	4567	19 Jan	0.16					15 Apr	-0.40							86.59	-0.56	I
47	Telashi Lake	63.15	4805	4 Nov	0.19					27 May	0.86							203.94	0.67	I
48	Tu Co	428	4929	23 Nov	-0.52	1 Dec	-0.93*	13 May	2.11*	26 May	1.70**	8.47	-0.41	163.24	3.04	12.65	-0.41	184.35	2.22**	I
49	Tuosu Lake	137.76	2805	24 Dec	0.17					25 Mar	-0.06							90.24	-0.23	III
50	Urru Co	362.52	4554	3 Jan	0.01					22 Apr	0.48							109.00	0.47	I

51	Xuejing Lake	72.73	4807	22 Oct	0.64**					11 Jun	-0.26							232.47	-0.91	I
52	Xuemei Lake	41.33	4873	26 Oct	0.30					24 Jun	0.34							240.94	0.04	I
53	Yaggain Co	97.41	4534	7 Dec	1.48**					19 Apr	0.10							132.82	-1.38**	I
54	Youbucuo Lake	63.19	4640	20 Dec	0.56*					15 Apr	-0.14							116.71	-0.70	I
55	Yuye Lake	126.36	4856	20 Oct	0.73**					14 Jun	-1.08							236.71	-1.81*	I
56	Zhari Namco	990.26	4612	27 Dec	0.64*	7 Jan	0.48	31 Mar	0.74	13 Apr	0.63	10.41	-0.17	83.29	0.26*	12.41	-0.11	106.12	-0.01	I
57	Zhaxi Co	47.47	4416	24 Nov	0.70**					13 Apr	-0.89**							139.71	-1.59**	I
58	Zige Tangco	225.55	4568	9 Dec	1.01**	15 Dec	0.94**	9 Apr	-0.17	24 Apr	-0.12	5.53	-0.07	115.47	-1.11*	14.88	0.05	135.88	-1.13*	I

Note. [a] Wan et al. (2014). [b] The altitudes of lakes are derived from Shuttle Radar Topography (SRTM) digital elevation model (DEM) data (http://srtm.csi.cgiar.org/SELECTION/inputCoord.asp). * Statistical significance at the 0.05 level (Mann-Kendall test). ** Statistical significance at the 0.01 level (Mann-Kendall test).

Appendix B

Table B1. *Lake Ice Phenology Statistics From 2001 to 2017 (FUS: Freeze-up Start, FUE: Freeze-up End, BUS: Break-up Start, BUE: Break-up End, FUD: Freeze-up Duration, BUD: Break-up Duration, CFD: Complete Freezing Duration, and ICD: Ice Cover Duration)*

		Mean[a]	Minimum	Maximum	Max-Min	Median	Standard deviation
Mean date/days	FUS**	30 Nov	20 Oct (Yuye Lake)	19 Jan (Taro Co)	90.47	29 Nov	21.57
	FUE*	16 Dec	15 Nov (Hoh Xil Lake)	22 Jan (Mapam Yumco)	68.48	13 Dec	17.81
	BUS*	16 Apr	18 Mar (Ngangze Co)	12 Jun (Hoh Xil Lake)	86.60	10 Apr	22.78
	BUE**	6 May	25 Mar (Tuosu Lake)	7 Jul (Gozha Co)	104.00	1 May	26.62
	FUD*	9.81	3.94 (Lagkor Co)	18.76 (Ngangla Ringco)	14.82	8.76	4.56
	BUD*	13.01	7.29 (Dong Co)	18.65 (Palung Co)	11.35	13.00	2.92
	CFD*	121.12	76.82 (Qinghai Lake)	209.65 (Hoh Xil Lake)	132.82	117.06	35.53
	ICD**	157.78	86.59 (Taro Co)	240.94 (Xuemei Lake)	154.35	147.74	42.99
Change rate (d yr^{-1})	FUS	0.53	-1.22 (Lexiewudan Co)	1.48 (Yaggain Co)	2.70		0.52
	FUE	0.54	-0.93 (Tu Co)	1.04 (Ngangze Co)	1.97		0.43
	BUS	0.58	-0.50 (Qinghai Lake)	2.11 (Tu Co)	2.61		0.69
	BUE	0.54	-1.63 (Bangkog Co)	4.25 (Lexiewudan Co)	5.88		0.92
	FUD	0.18	-0.41 (Tu Co)	0.41 (Sugan Lake)	0.82		0.20
	BUD	0.30	-0.80 (Ngangze Co)	0.43 (Qinghai Lake)	1.24		0.35
	CFD	0.68	-1.13 (Lagkor Co)	3.04 (Tu Co)	4.17		0.97
	ICD	0.90	-2.73 (Bangkog Co)	5.46 (Lexiewudan Co)	8.20		1.32

Note. [a] The mean change rates of lake ice phenology are mean absolute values. * Calculated from 18 lakes. ** Calculated from 58 lakes.